

# Occupation Dynamics of Floquet-Volkov States and Spectral Sum Rule

Xuanxi Cai<sup>∞,†</sup>, Changhua Bao<sup>∞,†</sup>, Benshu Fan<sup>∞,†,‡</sup>, Haoyuan Zhong,<sup>†</sup> Fei Wang,<sup>†</sup>  
 Shaohua Zhou,<sup>†</sup> Tianyun Lin,<sup>†</sup> Hongyun Zhang,<sup>†</sup> Pu Yu,<sup>†,¶</sup> Peizhe Tang,<sup>\*,§,‡</sup>  
 Wenhui Duan,<sup>†,¶,||</sup> and Shuyun Zhou<sup>\*,†,¶</sup>

<sup>†</sup>*State Key Laboratory of Low Dimensional Quantum Physics and Department of Physics, Tsinghua University, Beijing 100084, P.R. China*

<sup>‡</sup>*Max Planck Institute for the Structure and Dynamics of Matter, Center for Free-Electron Laser Science, Hamburg 22761, Germany*

<sup>¶</sup>*Frontier Science Center for Quantum Information, Beijing 100084, P.R. China*

<sup>§</sup>*School of Materials Science and Engineering, Beihang University, Beijing 100191, P.R. China*

<sup>||</sup>*Institute for Advanced Study, Tsinghua University, Beijing 100084, P.R. China*

E-mail: peizhet@buaa.edu.cn; syzhou@mail.tsinghua.edu.cn

## Abstract

Time-periodic light fields can dress electronic states in quantum materials, forming Floquet states whose dynamic occupation determines transient material properties. Here by using time- and angle-resolved photoemission spectroscopy (TrARPES), we reveal the transient occupation of Floquet-Volkov states in two semiconductors, black phosphorus and MoSe<sub>2</sub>. While the occupation of the light-induced sidebands, directly reflected by TrARPES spectral weight, strongly depends on the driving field, we find that the total spectral weight obtained by summing up all sidebands is conserved upon

below-gap driving. Our work provides critical insights into the Floquet population dynamics, which are essential for light-field tailoring of transient material properties.

## Keywords

Floquet engineering, electronic occupation, spectral sum rule, time-resolved ARPES

Floquet engineering, the control of quantum materials through time-periodic drive, has emerged as a powerful paradigm for creating non-equilibrium states of matter with tailored properties.<sup>1-5</sup> This approach is rooted in a fundamental analogy with the Bloch states:<sup>6</sup> the spatially-periodic potential in crystals leads to Bloch bands which are periodic in the momentum space. Similarly, a time-periodic drive dresses the Bloch states inside the crystal, forming energy-periodic Floquet-Bloch states.<sup>7,8</sup> Such light-field dressed states,  $|\psi_\alpha(t)\rangle$ , are superpositions of multiple “photon-dressed” states  $|u_\alpha^n\rangle$ , expressed as  $|\psi_\alpha(t)\rangle = \sum_n |u_\alpha^n\rangle e^{-i(\epsilon_\alpha + n\hbar\omega)t/\hbar}$ . The eigen energies of these constituent states are different by integer multiples of the drive photon energy  $n\hbar\omega$ . The interaction of these Floquet states with the time-periodic potential can further open up energy gaps and modify the non-equilibrium properties of target materials, leading to light-field tailored electronic structure<sup>9-15</sup> and emergent phenomena such as the light-induced anomalous Hall effect,<sup>16,17</sup> the optical Stark effect,<sup>18-20</sup> and tailored optical nonlinearities.<sup>21,22</sup>

Crucially, the resulting transient electronic, transport, and optical properties are governed by the non-equilibrium occupation of these Floquet states.<sup>16,23-25</sup> Unlike the equilibrium state, where bands below the Fermi energy are completely filled, the Floquet regime creates a distinct electronic structure, where the valence band (VB) and its multiple sidebands, both above and below the Fermi energy, coexist as a coherent superposition. This results in a complex population landscape where each state is only partially filled and dynamically evolving with the drive.<sup>26-29</sup> In addition, as solid-state materials under laser driving are open

systems coupled with baths, the Floquet occupation dynamics often involves complicated competition between the laser driving and the relaxation of photo-excited electrons in the target materials.<sup>23,24,26,28,30–38</sup> Thus, in sharp contrast to equilibrium quantum statistics, which guarantees the conservation of total electron spectral weight, the total occupation of these Floquet sidebands in non-equilibrium is not always guaranteed to be conserved<sup>26,31</sup> due to strong coupling between these states and the baths [see discussions in Supporting Information (SI)]. Therefore, it is critical to characterize the intricate population dynamics and investigate under what conditions a spectral sum rule can be established.

Here we directly reveal the population dynamics of light-field dressed states in two semiconductors, black phosphorus and 2H-MoSe<sub>2</sub>, by using time- and angle-resolved photoemission spectroscopy (TrARPES). Under intense pumping, we observe sidebands up to the third order, and a complete depletion of the VB. Interestingly, while the occupation of each sideband strongly depends on the driving field and the delay time, we observe isosbestic points in the TrARPES spectra upon below-gap pumping, indicating a spectral sum rule, namely, conservation of the total TrARPES spectral weight at a fixed momentum. Such a sum rule is violated by above-gap pumping that involves direct optical transitions in addition to coherent light-matter coupling. Our work provides fundamental insights into the occupation dynamics of Floquet states, which are crucial for the modulation of ultrafast transport and opto-electronic properties in light-engineered quantum materials.

Figure 1a shows a schematic of the TrARPES setup, where a mid-infrared (MIR) pulse at 160 meV is used as the drive (see Figure S1 in the SI for experimental geometry). The equilibrium electronic structures of black phosphorus along the armchair (AC) and zigzag (ZZ) directions are shown in Figure 1b, c. The dynamic occupation of light-field dressed states is reflected by comparing the TrARPES spectral weight  $S(\mathbf{k}) = \int I(\mathbf{k}, E)dE$  with the equilibrium state, where  $I(\mathbf{k}, E)$  is the TrARPES intensity,  $\mathbf{k}$  and  $E$  are electron momentum and energy, respectively. The TrARPES intensity is expressed as  $I(\mathbf{k}, E) \simeq A(\mathbf{k}, E)|M(\mathbf{k}, E)|^2 f(\mathbf{k}, E)$ , where  $A$ ,  $f$  denote spectral function and occupation function, respectively, and  $M$  is the

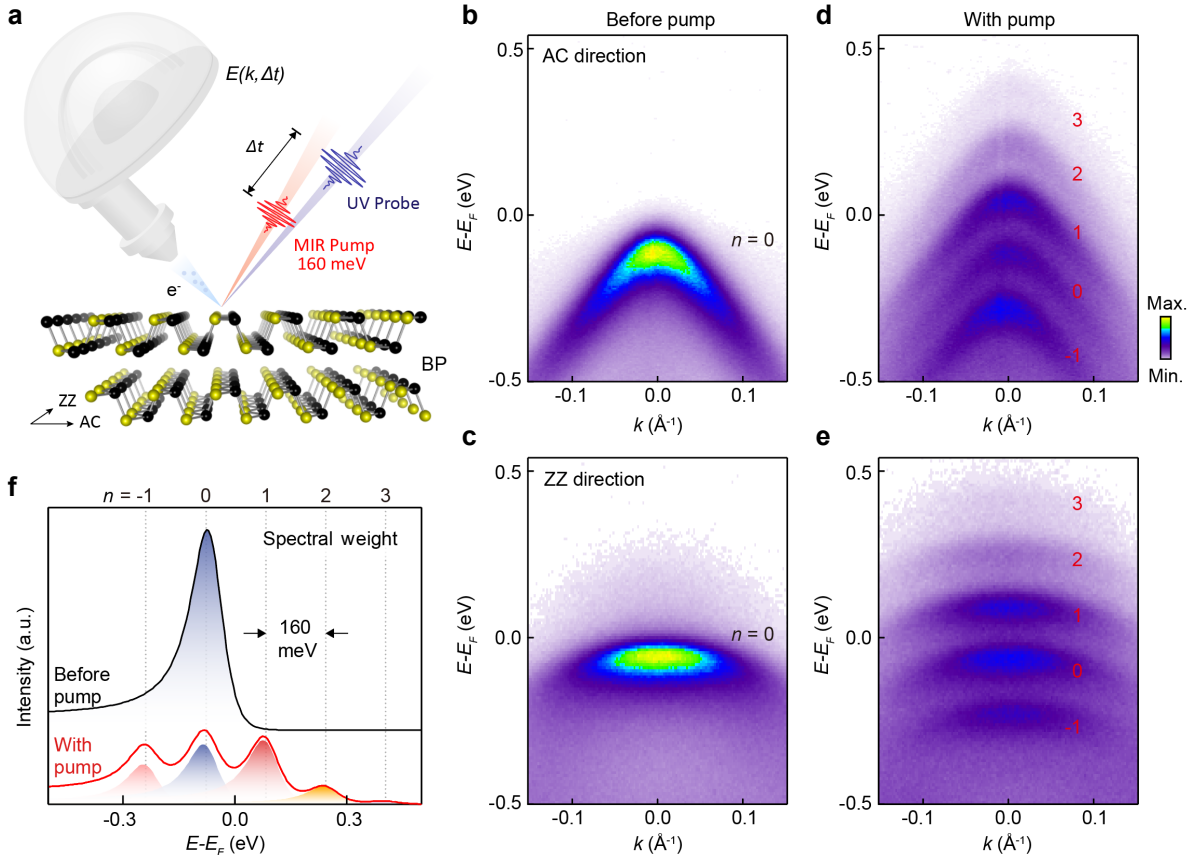


Figure 1: Light-induced sidebands and spectral weight redistribution in black phosphorus upon below-gap pumping. (a) Schematic of TrARPES setup with MIR pumping. (b, c) Dispersion images measured at  $\Delta t = -1$  ps along the AC (b) and ZZ (c) directions. (d, e) Dispersion images measured at  $\Delta t = 0$  along the AC (d) and ZZ (e) directions. (f) EDCs at  $k = 0$  for data in (c, e). The color-shaded areas are fitting peaks, which are used to extract the spectral weight for each individual peak. The pump has a photon energy of 160 meV and fluence of  $0.5 \text{ mJ/cm}^2$ . The pump is  $p$ -polarized, with polarization along ZZ direction (ZZ-pump) for (d) and polarization along AC direction (AC-pump) for (e).

dipole transition matrix element which is related to measurement geometry and irrelevant to occupation.<sup>39</sup> Under certain geometries, the dipole transition matrix element is similar between different dressed states, so that the extracted spectral weight reveals the dynamic occupation.

Upon below-gap pumping at a fluence of  $0.5 \text{ mJ/cm}^2$  (with corresponding peak field strength of  $1.1 \times 10^8 \text{ V/m}$ ), the intensity of the VB ( $n = 0$ ) clearly decreases, and multiple sidebands are clearly observed in Figure 1d, e. Here, the application of *p-pol.* pump (with non-zero out-of-plane light-field) leads to the interference between the Floquet and Volkov states,<sup>40–44</sup> thereby enhancing sideband intensity with occupation up to the third order ( $n = 3$ ) (see more details in Figure S1). In this work, we utilize various combinations of pump and probe polarizations, so that the Floquet optical selection rule guarantees that Floquet states and the related Floquet-Volkov states are clearly observed,<sup>45,46</sup> whose occupations are revealed by TrARPES intensity.

Figure 1f compares the energy distribution curves (EDCs) at the  $\Gamma$  point before and upon pumping, extracted from Figure 1c, e. The single peak in the equilibrium state becomes weaker upon pumping, with its spectral weight redistributed into sidebands displaced by the drive photon energy of 160 meV. The reduced spectral intensity of the  $n = 0$  VB indicates that there is less electron filling, namely, the VB is only partially occupied, which is in sharp contrast to the occupation of the equilibrium state. The spectral weight of these Floquet-Volkov states strongly depends on the pump strength, scaling with the square of the  $n$ -th Bessel function  $J_n^2(\gamma)$ . Here, the parameter  $\gamma$  depends on the electronic structures of the VBs, the properties of the pumping laser, and the velocity of photoelectrons (see details in Methods). At a pump fluence of  $0.5 \text{ mJ/cm}^2$ , the population is slightly inverted, which is indicated by the slightly higher intensity for the first-order  $n = 1$  sideband (red shaded area in Figure 1f) than the  $n = 0$  band (blue shaded area). Under stronger pumping at  $1.1 \text{ mJ/cm}^2$ , the  $n = 0$  VB is nearly depleted, and the spectral weight is almost entirely redistributed into the  $|n| \geq 1$  sidebands (Figure S2). Such a drastic population modulation could reshape

electronic properties, e.g., by flipping fermionic interactions.<sup>47</sup> In previous works,<sup>10,48,49</sup> we have demonstrated light-field induced band renormalization, and here we focus on another crucial and fundamental question, the dynamical occupation of these transient sidebands.

The temporal evolution of Floquet-Volkov spectral weight encodes critical information about the underlying transient occupation. Figure 2a-e shows snapshots of dispersion images measured at five representative delay times (marked in Figure 2f). Figure 2g shows the corresponding EDCs at the  $\Gamma$  point. Interestingly, the EDCs at different delay times always intersect at two points as pointed by red arrows, which is analogous to isosbestic points in chemical reactions,<sup>50-52</sup> Mott transition,<sup>53</sup> and structural transition<sup>54</sup> in solid states. Such isosbestic points are indications of the conservation of the total populations where there is inter-conversion between different species/states.<sup>51,52</sup> The observation of isosbestic points here indicates the inter-conversion between the VB and sidebands with  $|n| \geq 1$ , and possible spectral weight conservation (see more discussion in SI).

The Floquet-Volkov spectral weight  $S_{FV}(\mathbf{k})$  is experimentally defined as the total TrARPES spectral weight by summing up the spectral weight of the VB  $S_{n=0}(\mathbf{k})$  and its sidebands  $S_{n \neq 0}(\mathbf{k})$  at a fixed momentum  $\mathbf{k}$ ,

$$S_{FV}(\mathbf{k}) = \sum_n S_n(\mathbf{k}) \quad (1)$$

The spectral weight for each sideband  $S_n(\mathbf{k})$  is extracted by integrating TrARPES intensity  $I_n(\mathbf{k}, E)$  over electron energy  $E$  (shaded area in Figure 2g). Figure 2h shows the extracted spectral weight for each sideband at different delay times, which changes with delay time due to the different field strength. Interestingly, the total spectral weight, summed over all sidebands ( $n = 0$  and  $n \neq 0$ ), is nearly conserved and matches the unpumped spectral weight (red dashed line). Theoretically, we use the Floquet theory to describe Floquet-Volkov interference, where the spectral weight of each sideband is simplified as a Bessel function without considering the coupling with the baths (see details in SI). Under this approximation, we

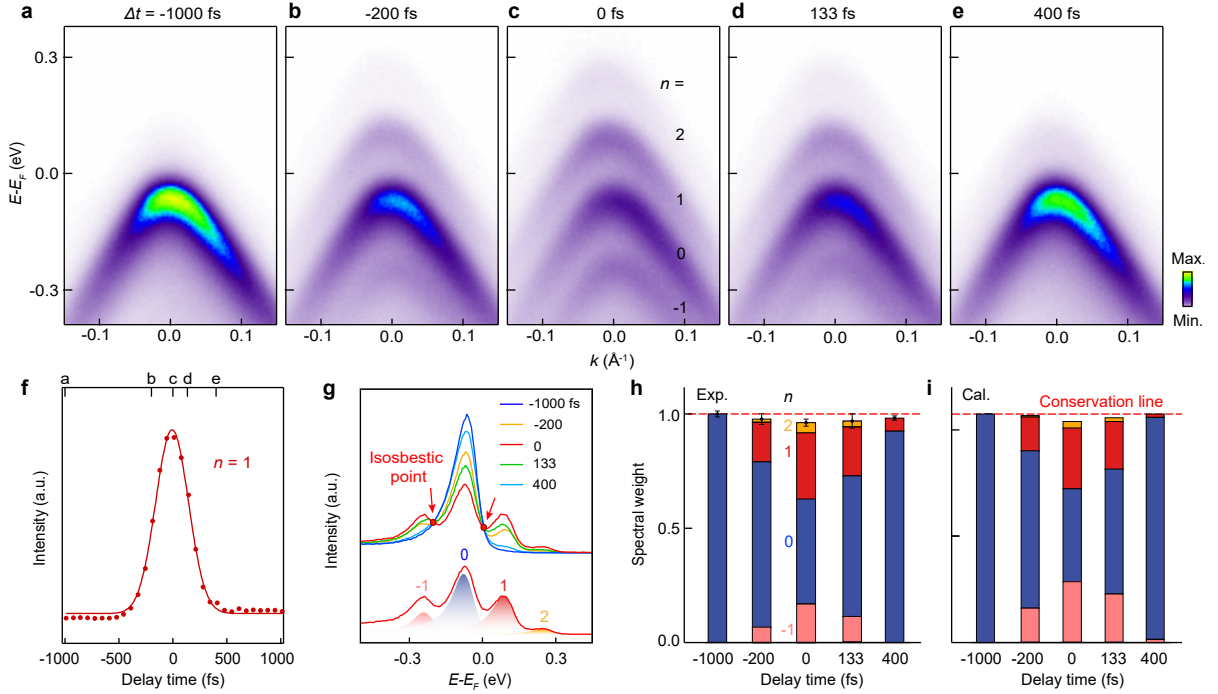


Figure 2: Observation of spectral weight conservation in black phosphorus. (a-e) Dispersion images measured along the direction at  $30^\circ$  from the AC direction of black phosphorus with  $p$ - $pol.$  at different delay times. The pump photon energy is 160 meV, and the pump fluence is  $0.32 \text{ mJ/cm}^2$ . (f) Intensity of  $n = 1$  sideband as a function of the delay time. (g) EDCs at  $k = 0$  from data in (a-e), and fitting of the EDC at  $\Delta t = 0$  (bottom curve). (h) Extracted spectral weight for different sidebands at different delay times from EDCs in (g). The error bars are for the total spectral weight and are estimated via standard uncertainty propagation from the fitting parameters. (i) Calculated spectral weight for  $n = 0, \pm 1, 2$  sidebands at different delay times.

model the redistribution of spectral weight among different sidebands and reproduce its conservation, as shown in Figure 2i. The qualitative agreement between simulated results and TrARPES measurements shows that a spectral sum rule holds, reflecting conserved occupations of light-dressed states. The conservation of total spectral weight and the presence of isosbestic points are also observed for different pump fluences (Figure S3) and in pure Floquet states under *s-pol.* pumping with weaker sidebands (Figure S4). Moreover, the spectral sum rule also holds for non-high-symmetry  $k$  points in addition to the  $\Gamma$  point (Figure S5).

The spectral sum rule is also observed in 2H-MoSe<sub>2</sub> upon pumping at 311 meV, which is far below its band gap of 1.1 eV.<sup>55</sup> Figure 3a shows an overview of the electronic structure using an advanced high-photon-energy light source.<sup>56</sup> Clear sidebands are observed around the K valley for both *s-pol.* and *p-pol.* pump (Figure 3b-g). In both cases, the pump polarization has a non-zero out-of-plane field component, which is larger for *p-pol.* pump, leading to stronger Floquet-Volkov sidebands in Figure 3d. Interestingly, a similar EDC analysis at the K point shows that the total spectral weight is conserved (Figure 3h, i), suggesting that the spectral sum rule also holds for 2H-MoSe<sub>2</sub> upon below-gap pumping.

We further explore the spectral sum rule by tuning pump photon energy across the band gap. Our results reveal a breakdown of the spectral sum rule for the light-induced valence sidebands once an optical transition to the conduction band (CB) is activated. Figure 4 shows a comparison of the spectral weight for valence sidebands of black phosphorus under below-gap (see schematic in Figure 4a) to above-gap pumping (Figure 4b). For below-gap pumping, the dispersion images at various pump photon energies show that the Floquet-Volkov spectral weight is conserved (Figure 4c-g). In contrast, upon above-gap AC-pumping (Figure 4h-k), such conservation is violated, which is supported by the analysis in Figure 4p (indicated by blue arrows). This breakdown occurs because above-gap AC-pump activates photo-excitation into the CB in accordance with the optical selection rule.<sup>57</sup> As shown by the population of CB in Figure 4l-o and Figure S6, electrons are not only redistributed among the sidebands, but are also transiently excited to the CB. This additional excitation

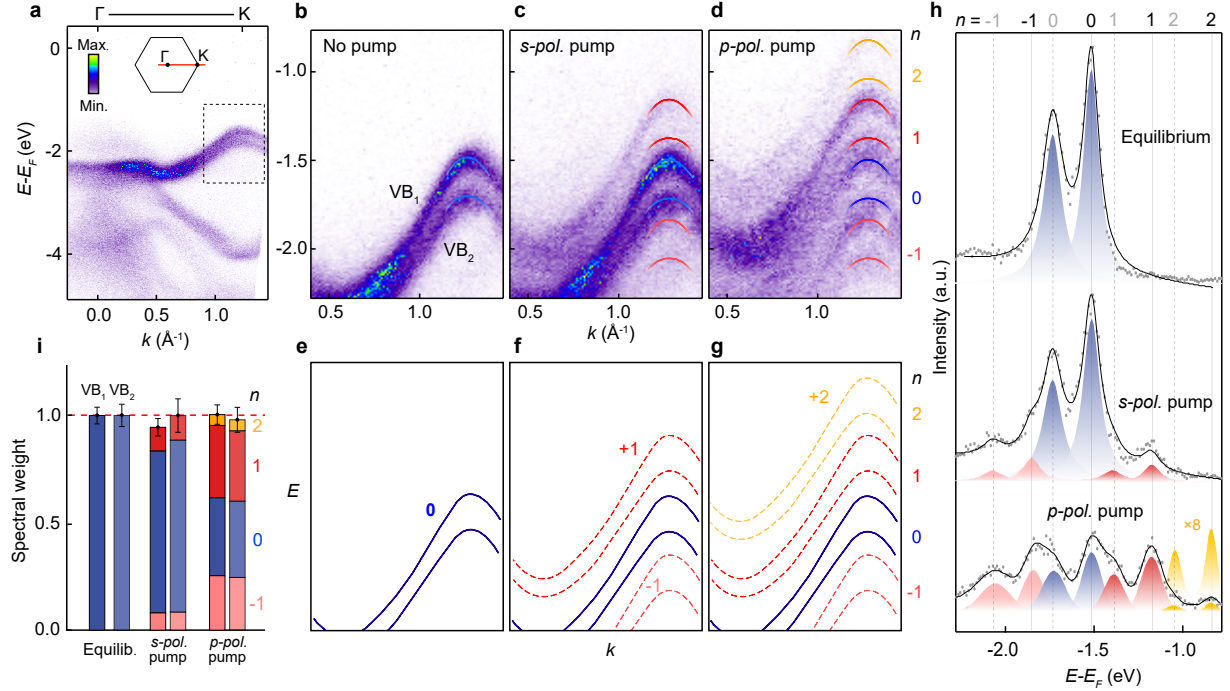


Figure 3: Observation of spectral weight conservation in MoSe<sub>2</sub>. (a) Dispersion image of bulk MoSe<sub>2</sub> measured along the  $\Gamma$ -K direction. The dashed box marks the band structure at the K valley, which is the main focus. (b-d) Dispersion images measured around the K valley without pump (b), with *s-pol.* (c) and *p-pol.* (d) pump. The pump photon energy is 311 meV and the pump fluence is 2.5 mJ/cm<sup>2</sup>. (e-g) Corresponding dispersions for data shown in (b-d). (h) EDCs at the K point for data shown in (b-d) and fitting results to extract the individual spectral weight. (i) Extracted spectral weight for different sidebands from EDC analysis in (h).

channel is responsible for the non-conservation of the total Floquet-Volkov spectral weight for the valence sidebands. In addition, we also note that for above-gap ZZ-pump where the direct interband transition is forbidden,<sup>57</sup> the Floquet-Volkov spectral weight is conserved (Figure S7).

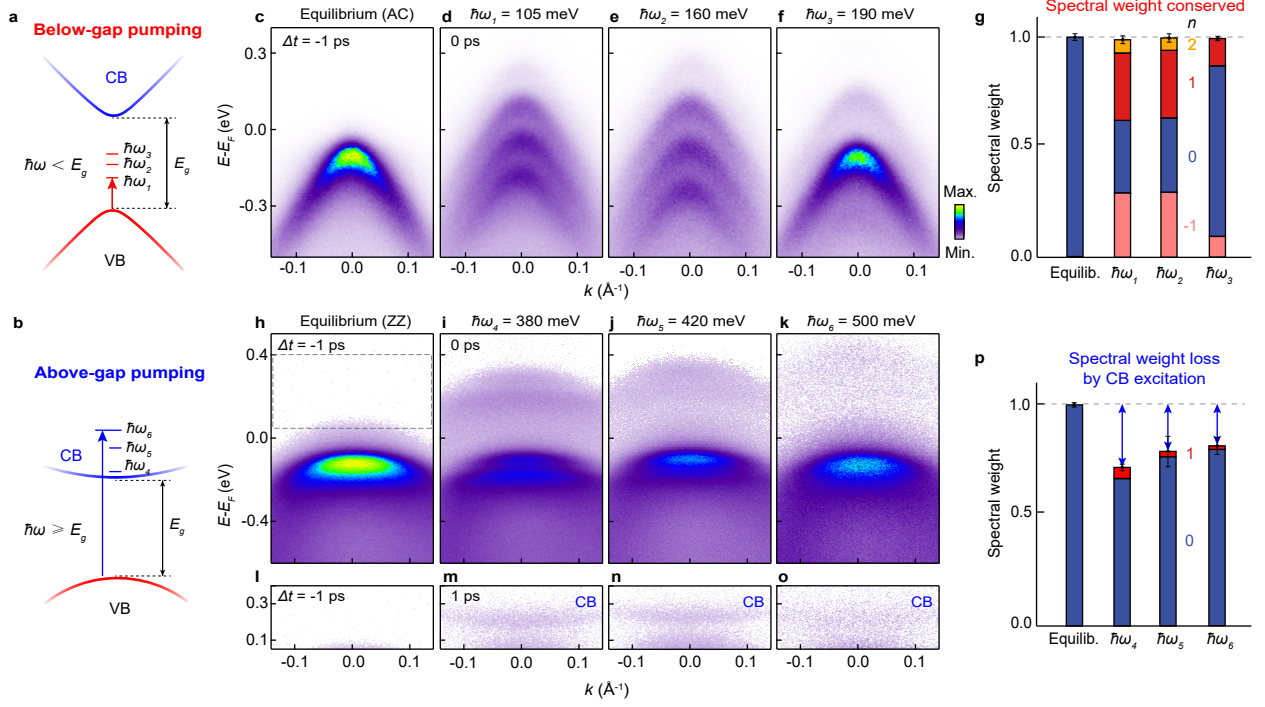


Figure 4: Conservation of spectral sum rule upon below-gap pumping, and violation of spectral sum rule upon above-gap pumping in black phosphorus. (a, b) A schematic illustration for the band structure and pump photon energies below the band gap  $E_g$  (a) and above the band gap (b). (c-f) Dispersion images measured along AC direction at  $\Delta t = -1$  ps (c) and at  $\Delta t = 0$  ps with three different pump photon energies (d-f). The pump is ZZ-pump ( $p$ -pol.) and the pump fluences are 0.29, 0.26 and 0.20 mJ/cm<sup>2</sup>, respectively. (g) Extracted spectral weight at the  $\Gamma$  point from data in (c-f). (h-k) Dispersion images measured along the ZZ direction at  $\Delta t = -1$  ps (h) and at  $\Delta t = 0$  ps with three different pump photon energies larger than the band gap (i-k). The pump is AC-pump ( $p$ -pol.) and the pump fluence is 0.7 mJ/cm<sup>2</sup>. (l-o) Zoomed-in dispersion images at  $\Delta t = -1$  ps (l) and at  $\Delta t = 1$  ps for three different above-gap pump photon energies (m-o). (p) Extracted spectral weight at the  $\Gamma$  point from data in (h-k).

The dynamic occupation of Floquet-Volkov states is manifested in the transfer of spectral weight among Floquet-Volkov sidebands and the conservation of the total spectral weight. Within the Floquet-Volkov description, the  $n$ -th sideband is characterized by the Floquet-Volkov coefficient  $c_n$ , with a sideband weight given by  $|c_n|^2 = J_n^2(|\gamma|)$ . Here,  $\gamma = \beta - \alpha$  is a

dimensionless parameter that characterizes the interference between the Floquet and Volkov states, where  $\beta$  describes the Floquet dressing of the initial state and  $\alpha$  the Volkov dressing of the photoelectron (see details in Methods). The  $n$ -th Bessel function  $J_n$ , which are tunable by the pumping strength, corresponds to the amplitudes of the harmonics of the Floquet wave functions.<sup>31</sup> Under below-gap pumping, where single photon absorption is suppressed, the sum of  $J_n^2$  over the Floquet index  $n$  is unity, as observed in both black phosphorus and MoSe<sub>2</sub>. In contrast, above-gap pumping may activate direct optical transitions, populating the CB with carriers and thereby diminishing the occupation of the VB and its sidebands. This leads to the violation of the spectral sum rule. We note an exception in black phosphorus when measured along the AC direction with AC-pump: even for below-gap pumping, the total spectral weight is not conserved around the  $\Gamma$  point (Figure S8). This arises from the Floquet matrix element effect,<sup>45,46</sup> which modulates the TrARPES intensity such that the measured spectral weight deviates from the true electronic occupation. This is purely a detection-related phenomenon; in principle, the total occupation of the Floquet–Volkov states still remains conserved. We also note that in the sub-cycle regime, the coherent light field can induce momentum shifts of spectral weight or the entire bands,<sup>29,58–60</sup> potentially leading to a breakdown of the sum rule. Such effects require ultrashort probe pulses and are beyond the scope of the present study.

In summary, we reveal the occupation dynamics of Floquet-Volkov states in two semiconductors. We find that below-gap pumping conserves the total spectral weight, establishing a spectral sum rule. This conservation indicates that electron occupation is preserved during light-field dressing, involving interconversion between the  $n = 0$  and  $n \neq 0$  states, and suggests negligible bath-mediated particle exchange out of the valence band Floquet manifold on the ultrafast timescale under below-gap pumping, although coherent energy exchange with the driving field remains essential. In contrast, above-gap pumping may open an alternative channel by directly exciting electrons into the CB, which diminishes the population of the light-dressed sidebands and breaks the spectral sum rule. Spectral sum rules are important

across different fields of physics, from particle physics<sup>61</sup> to condensed matter physics.<sup>62,63</sup> For instance, the sum rule in X-ray magnetic circular dichroism (XMCD) is used to determine the orbital or spin moments.<sup>63</sup> Our demonstration of the Floquet spectral sum rule, combined with the direct observation of transient occupation of light-field dressed states, suggests that below-gap pumping creates pure light-field dressed states, and provides useful insights for understanding and controlling the ultrafast transport and optoelectronic properties of Floquet quantum materials.

## METHODS

### Sample preparation

High-quality single crystals of black phosphorus and MoSe<sub>2</sub> were grown by chemical vapour transport method. For black phosphorus, a mixture of red phosphorus lump (Alfa Aesar, 99.999%), tin grains (Aladdin,  $\geq 99.5\%$ ), and iodine crystals (Alfa Aesar, 99.9%) was heated to 600°C for 1 day in an evacuated silica tube. For MoSe<sub>2</sub>, Mo foil (Alfa Aesar, 99.95%) and Se ingot (Alfa Aesar, 99.99%) were mixed and heated to 900°C for 3 days. The as-grown MoSe<sub>2</sub> was then recrystallized using SeCl<sub>4</sub> (Aladdin, 99%) as the transporting agent under 980°C for 9 days. Millimeter-sized black phosphorus and MoSe<sub>2</sub> single crystals were obtained.

### TrARPES measurements

TrARPES measurements were performed in the home laboratory at Tsinghua University with a regenerative amplifier laser with a center wavelength of 800 nm (1.55 eV) and a pulse energy of 1.3 mJ, at a repetition rate of 10 kHz. The majority of the beam is used to drive the optical parametric amplifier. The MIR pump beam is generated by non-collinear differential frequency generation of the signal and idler of the optical parametric amplifier. The probe beam with a photon energy of 6.2 eV is generated by a three-step fourth-harmonic

generation process using beta barium borate crystals. The temporal scales of the MIR pump and the 6.2 eV probe are shown in Figure S9. The probe beam with a photon energy of 21.7 eV is generated via high harmonic generation by focusing the second harmonic (3.1 eV) of the fundamental beam into an Argon-filled gas cell.<sup>56</sup> The 21.7 eV beam (7th harmonic of 3.1 eV) is isolated from other harmonics by passing through an aluminium foil and a tin foil. The samples were cleaved and measured at a temperature of 80 K in an ultra-high vacuum chamber with a base pressure better than  $5 \times 10^{-11}$  Torr.

## The extraction of spectral weights

The spectral weights are extracted by fitting the EDCs with Lorentzian peaks multiplied by a Fermi–Dirac function plus a linear background. The EDCs are obtained by integrating over a momentum window of  $0.02 \text{ \AA}^{-1}$  around each  $k$  point. The spectral weight of each sideband  $S_n(\mathbf{k})$  is determined by integrating the corresponding fitting peak  $I_n(\mathbf{k}, E)$  over energy  $E$ . The associated error bars are estimated via standard uncertainty propagation from the fitting parameters.

## The simulation of spectral weights

In this work, we employ Floquet theory to calculate the spectral weight of the Floquet-Volkov state in black phosphorus. We begin by deriving the spectral weight for the Floquet and Volkov states, which subsequently allows us to determine the spectral weight of the Floquet-Volkov state.<sup>64</sup>

For the Floquet state, we consider the in-plane component of the vector potential  $\mathbf{A}_{\parallel}(t)$  of the pumping laser as

$$\begin{aligned} \mathbf{A}_{\parallel}(t) &= A_x(t)\hat{\mathbf{x}} + A_y(t)\hat{\mathbf{y}} \\ &= A_x \cos(\omega t)\hat{\mathbf{x}} + A_y \cos(\omega t)\hat{\mathbf{y}} \end{aligned} \tag{2}$$

where  $A_x$  and  $A_y$  are the amplitudes of the vector potential along  $x$  (ZZ) and  $y$  (AC) directions, and  $\omega$  is the frequency of the pumping laser. We consider the electronic structures

of black phosphorus in equilibrium to be well described by a parabolic band and incorporate the influence of the pumping laser using the Peierls substitution. Therefore, the effective Hamiltonian  $\hat{H}_\Gamma(t, p_\parallel)$  of the VB edge around the  $\Gamma$  point is given by

$$\begin{aligned}
\hat{H}_\Gamma(t, p_\parallel) &= \sum_{i=x,y} \frac{[p_i + eA_i(t)]^2}{2m_i} \\
&= \sum_{i=x,y} \left[ \frac{p_i^2}{2m_i} + \frac{ep_iA_i(t) + eA_i(t)p_i}{2m_i} + \frac{e^2A_i^2(t)}{2m_i} \right] \\
&\simeq \sum_{i=x,y} \left[ \frac{p_i^2}{2m_i} + \frac{eA_i(t)p_i}{m_i} \right]
\end{aligned} \tag{3}$$

where  $e$  is the charge of electron,  $p_i = \hbar k_i$  is the lattice momentum with  $\hbar$  as the reduced Planck constant, and  $m_i$  is the effective mass of the electron along the  $i$  direction. The higher-order terms are neglected. Applying eq 2, we can simplify  $\hat{H}_\Gamma(t, p_\parallel)$  as

$$\begin{aligned}
\hat{H}_\Gamma(t, p_\parallel) &= \sum_{i=x,y} \frac{p_i^2}{2m_i} + \frac{eA_x(t)p_xm_y + eA_y(t)p_ym_x}{m_xm_y} \\
&= \sum_{i=x,y} \frac{p_i^2}{2m_i} + \hbar\omega\beta \cos(\omega t) \\
&= \hat{H}_0(p_\parallel) + \hat{H}_I(t, \beta)
\end{aligned} \tag{4}$$

where  $\beta = \frac{e(A_xp_xm_y + A_yp_ym_x)}{\hbar\omega m_xm_y}$ . Using the Jacobi-Anger relation  $e^{-in \sin \theta} = \sum_m J_m(n)e^{-im\theta}$ , we find that the evolution of the Floquet state is governed by  $\hat{H}_I(t, \beta) = \hbar\omega\beta \cos(\omega t)$ , leading to a wavefunction of the Floquet state given by

$$\begin{aligned}
\Psi^F(t) &= \exp \left[ -\frac{i}{\hbar} \int dt \hat{H}_I(t, \beta) \right] \Psi(t_0) \\
&= \exp [-i\beta \sin(\omega t)] \Psi(t_0) \\
&= \Psi(t_0) \sum_{m=-\infty}^{+\infty} J_m(\beta) e^{-im\omega t}
\end{aligned} \tag{5}$$

where  $\Psi(t_0)$  is the unperturbed wavefunction and  $J_m(x)$  is the  $m$ -th Bessel function of the first kind. Now we define the Floquet coefficient  $b_m$  as  $J_m(\beta)$ . If we do not consider the

dissipative effects,<sup>40</sup> the spectral weight of the  $m$ -th Floquet sideband is  $I_m^F = |b_m|^2$ .

The Volkov state arises from the interference between the pumping laser and photoexcited electrons, leading to a Hamiltonian of  $\hat{H}_V(t) = ev_z A_z(t) = ev_z A_z \cos(\omega t)$ , where  $v_z$  is the out-of-plane electron velocity and  $A_z$  is the vertical component of the vector potential of the pumping laser. Similar to the Floquet state, we obtain the time-dependent evolution of the Volkov state as

$$\begin{aligned}\Psi^v(t) &= \exp\left[-\frac{i}{\hbar} \int dt \hat{H}_V(t)\right] \Psi_k(t_0) \\ &= \exp\left[-\frac{i}{\hbar} \frac{eA_z v_z \sin(\omega t)}{\omega}\right] \Psi_k(t_0) \\ &= \Psi_k(t_0) \sum_{n=-\infty}^{+\infty} J_n(\alpha) e^{-in\omega t}\end{aligned}\quad (6)$$

where  $\Psi_k(t_0)$  is the free electron wavefunction and  $\alpha = \frac{eA_z v_z}{\hbar\omega}$ . The Volkov coefficient  $a_n$  is defined as  $J_n(\alpha)$ . For the Volkov state, the spectral weight of the  $n$ -th Volkov energy level is  $I_n^V = |a_n|^2$ .

For the Floquet-Volkov state, the interference between Floquet states and Volkov states should be considered. Herein, we can define the Floquet-Volkov coefficient<sup>64</sup> as

$$c_q \equiv \sum_{n,m}^{m-n=q} a_n^\dagger b_m = \sum_{n',m}^{m+n'=q} a_{-n'}^\dagger b_m \quad (7)$$

where the  $(n, m)$  summation is a discrete convolution and  $a_{-n'}^\dagger = (-1)^{n'} a_{n'}$ . Using the summation theorem for the Bessel function of the first kind,<sup>65</sup> the Floquet-Volkov coefficient becomes

$$\begin{aligned}c_q &= \sum_{n',m}^{m+n'=q} (-1)^{n'} J_{n'}(\alpha) J_m(\beta) \\ &= \sum_{n'} J_{-n'}(\alpha) J_{q-n'}(\beta) \\ &= \sum_{n'} J_{n'}(\alpha) J_{q+n'}(\beta) \\ &= \left(\frac{\gamma}{|\gamma|}\right)^q J_q(|\gamma|)\end{aligned}\quad (8)$$

where  $\gamma = \beta - \alpha$ . So for the Floquet-Volkov state, the spectral weight of the  $q$ -th sideband is  $I_q^{FV} = |c_q|^2$ .

In our calculations of the spectral weight for the Floquet-Volkov state (see Figure 2i in the main text and Figure S3h), the photon energy of the pumping laser is set at  $\hbar\omega = 160$  meV, and the effective mass of the electron  $m_x$  ( $m_y$ ) along the  $x$  ( $y$ ) direction is  $0.81m_e$  ( $0.13m_e$ ), where  $m_e$  is the electron mass. For pump-probe experiments with different delay times upon ZZ-pump (*p-pol.*, see Figure S1a for experimental geometry), we employ the electric field as  $E(t) = (E_x, E_z)e^{-\frac{(t/\tau)^2}{2}}$ , where  $\tau = 222$  fs and  $t$  represents different delay times as  $-1000$ ,  $-200$ ,  $0$ ,  $133$  and  $400$  fs. The parallel and vertical electric field amplitudes  $E_x$  and  $E_z$  with respect to the sample surface are  $3.35 \times 10^7$  V/m and  $6.4 \times 10^7$  V/m, respectively. The vector potential of the pumping laser  $A_{x,z}$  is calculated via  $E_{x,z}/\omega$ , and the electron velocity  $v_z$  in the out-of-plane direction is  $7.7 \times 10^5$  m/s. In this case, the corresponding  $|\gamma|$  is 0, 0.844, 1.267, 1.059, and 0.250 at different delay times.

To simulate Floquet-Volkov spectral weight under different pump fluences (as shown in Figure S3h), we determine the vector potential  $A_{x,z}$  from the pump fluences  $F$  used in the pump-probe experiments ( $F = 0, 0.081, 0.156, 0.207$  and  $0.276$  mJ/cm<sup>2</sup>), with the corresponding  $|\gamma|$  as 0, 0.640, 0.889, 1.024 and 1.182, respectively.

## Supporting Information Available

This material is available free of charge via the internet at <http://pubs.acs.org>.

Experimental geometry, complete occupation depletion of the original valence band, Floquet spectral sum rule holds under different pump fluences, Floquet spectral sum rule for pure Floquet-Bloch states, underlying mechanism for observing isosbestic points in the Floquet spectrum, conservation of spectral weight for both high-symmetry and non-high-symmetry  $k$  points, spectral weight dynamics upon above-gap AC-pumping in black phosphorus, conservation of spectral weight for above-gap ZZ-pumping in black phosphorus, violation of

Floquet spectral sum rule due to Floquet matrix element effect, temporal scales of the pump and probe pulses, and more discussions on the spectral weights. (PDF).

## AUTHOR INFORMATION

### Author Contributions

<sup>∞</sup> X.C., C.B. and B.F. contributed equally to this work.

Shuyun Z. conceived the research project. X.C., C.B., Haoyuan Z. and Shaohua Z. performed the TrARPES measurements and analyzed the data. F.W. and Haoyuan Z. grew the black phosphorus and MoSe<sub>2</sub> single crystals. B.F., P.T. and W.D. performed the theoretical analysis and calculation. T.L., Hongyun Z. and P.Y. contributed to the data analysis and discussions. X.C. and Shuyun Z. wrote the manuscript, and all authors contributed to the discussions and commented on the manuscript.

### Notes

The authors declare no competing financial interest.

### Acknowledgment

This work is supported by the National Natural Science Foundation of China (Grants No. 12234011, 12421004), Tsinghua University Initiative Scientific Research Program (Grant No. 20251080106), National Natural Science Foundation of China (52388201, 12327805, 12374053), the National Key Basic Research and Development Program of China (Grants No. 2024YFA1409100), and the New Cornerstone Science Foundation through the XPLOER PRIZE.

## References

- (1) Oka, T.; Kitamura, S. Floquet engineering of quantum materials. *Annu. Rev. Condens. Matter Phys.* **2019**, *10*, 387–408.
- (2) Basov, D.; Averitt, R.; Hsieh, D. Towards properties on demand in quantum materials. *Nat. Mater.* **2017**, *16*, 1077–1088.
- (3) Rudner, M. S.; Lindner, N. H. Band structure engineering and non-equilibrium dynamics in Floquet topological insulators. *Nat. Rev. Phys.* **2020**, *2*, 229–244.
- (4) De La Torre, A.; Kennes, D. M.; Claassen, M.; Gerber, S.; McIver, J. W.; Sentef, M. A. Colloquium: Nonthermal pathways to ultrafast control in quantum materials. *Rev. Mod. Phys.* **2021**, *93*, 041002.
- (5) Bao, C.; Tang, P.; Sun, D.; Zhou, S. Light-induced emergent phenomena in 2D materials and topological materials. *Nat. Rev. Phys.* **2022**, *4*, 33–48.
- (6) Ashcroft, N. W.; Mermin, N. D. *Solid State Physics*; Cengage Learning, 2022.
- (7) Shirley, J. H. Solution of the Schrödinger equation with a Hamiltonian periodic in time. *Phys. Rev.* **1965**, *138*, B979–B987.
- (8) Oka, T.; Aoki, H. Photovoltaic Hall effect in graphene. *Phys. Rev. B* **2009**, *79*, 081406.
- (9) Wang, Y.; Steinberg, H.; Jarillo-Herrero, P.; Gedik, N. Observation of Floquet-Bloch states on the surface of a topological insulator. *Science* **2013**, *342*, 453–457.
- (10) Zhou, S.; Bao, C.; Fan, B.; Zhou, H.; Gao, Q.; Zhong, H.; Lin, T.; Liu, H.; Yu, P.; Tang, P.; others Pseudospin-selective Floquet band engineering in black phosphorus. *Nature* **2023**, *614*, 75–80.

- (11) Wang, F.; Cai, X.; Tang, X.; Lu, J.; Chen, W.; Sheng, T.; Feng, R.; Zhong, H.; Zhang, H.; Yu, P.; others Observation of Floquet-induced gap in graphene. *Nat. Mater.* **2026**, <https://doi.org/10.1038/s41563-026-02549-y>.
- (12) Wang, F.; Cai, X.; Chen, W.; Lu, J.; Sheng, T.; Tang, X.; Li, J.; Zhang, H.; Zhou, S. Robust Floquet-induced gap in irradiated graphite. *Chin. Phys. Lett.* **2026**, *43*, 050705.
- (13) Bielinski, N.; Chari, R.; May-Mann, J.; Kim, S.; Zwettler, J.; Deng, Y.; Aishwarya, A.; Roychowdhury, S.; Shekhar, C.; Hashimoto, M.; others Floquet–Bloch manipulation of the Dirac gap in a topological antiferromagnet. *Nat. Phys.* **2025**, *21*, 458–463.
- (14) Pareek, V.; Bacon, D. R.; Zhu, X.; Chan, Y.-H.; Bussolotti, F.; Menezes, M. G.; Chan, N. S.; Urquizo, J. P.; Watanabe, K.; Taniguchi, T.; others Driving Floquet physics with excitonic fields. *Nat. Phys.* **2026**, *22*, 209–217.
- (15) Wang, F.; Cai, X.; Xiao, T.; others Floquet engineering enabled by charge density wave transition. *arXiv preprint* **2025**, Submitted 21 Oct 2025. <https://arxiv.org/abs/2510.18323> (accessed 2026-05-07).
- (16) Kitagawa, T.; Oka, T.; Brataas, A.; Fu, L.; Demler, E. Transport properties of nonequilibrium systems under the application of light: Photoinduced quantum Hall insulators without Landau levels. *Phys. Rev. B* **2011**, *84*, 235108.
- (17) McIver, J. W.; Schulte, B.; Stein, F.-U.; Matsuyama, T.; Jotzu, G.; Meier, G.; Cavalleri, A. Light-induced anomalous Hall effect in graphene. *Nat. Phys.* **2020**, *16*, 38–41.
- (18) Sie, E. J.; McIver, J. W.; Lee, Y. H.; Fu, L.; Kong, J.; Gedik, N. Valley-selective optical Stark effect in monolayer WS<sub>2</sub>. *Nat. Mater.* **2015**, *14*, 290–294.
- (19) Sie, E. J.; Lui, C. H.; Lee, Y.-H.; Fu, L.; Kong, J.; Gedik, N. Large, valley-exclusive Bloch-Siegert shift in monolayer WS<sub>2</sub>. *Science* **2017**, *355*, 1066–1069.

- (20) Kobayashi, Y.; Heide, C.; Johnson, A. C.; Tiwari, V.; Liu, F.; Reis, D. A.; Heinz, T. F.; Ghimire, S. Floquet engineering of strongly driven excitons in monolayer tungsten disulfide. *Nat. Phys.* **2023**, *19*, 171–176.
- (21) Shan, J.-Y.; Ye, M.; Chu, H.; Lee, S.; Park, J.-G.; Balents, L.; Hsieh, D. Giant modulation of optical nonlinearity by Floquet engineering. *Nature* **2021**, *600*, 235–239.
- (22) Zhang, X.; Carbin, T.; Culver, A. B.; Du, K.; Wang, K.; Cheong, S.-W.; Roy, R.; Kogar, A. Light-induced electronic polarization in antiferromagnetic  $\text{Cr}_2\text{O}_3$ . *Nat. Mater.* **2024**, *23*, 790–795.
- (23) Sato, S.; McIver, J.; Nuske, M.; Tang, P.; Jotzu, G.; Schulte, B.; Hübener, H.; De Giovannini, U.; Mathey, L.; Sentef, M.; others Microscopic theory for the light-induced anomalous Hall effect in graphene. *Phys. Rev. B* **2019**, *99*, 214302.
- (24) Sato, S.; Tang, P.; Sentef, M.; De Giovannini, U.; Hübener, H.; Rubio, A. Light-induced anomalous Hall effect in massless Dirac fermion systems and topological insulators with dissipation. *New J. Phys.* **2019**, *21*, 093005.
- (25) Gao, Q.; Ren, Y.; Niu, Q. DC current generation and power feature in strongly driven Floquet-Bloch systems. *Phys. Rev. Res.* **2022**, *4*, 013216.
- (26) Seetharam, K. I.; Bardyn, C.-E.; Lindner, N. H.; Rudner, M. S.; Refael, G. Controlled population of Floquet-Bloch states via coupling to Bose and Fermi baths. *Phys. Rev. X* **2015**, *5*, 041050.
- (27) Seetharam, K.; Titum, P.; Kolodrubetz, M.; Refael, G. Absence of thermalization in finite isolated interacting Floquet systems. *Phys. Rev. B* **2018**, *97*, 014311.
- (28) Iadecola, T.; Neupert, T.; Chamon, C. Occupation of topological Floquet bands in open systems. *Phys. Rev. B* **2015**, *91*, 235133.

- (29) Ito, S.; Schüler, M.; Meierhofer, M.; Schlauderer, S.; Freudenstein, J.; Reimann, J.; Afanasiev, D.; Kokh, K.; Tereshchenko, O.; Gütde, J.; others Build-up and dephasing of Floquet–Bloch bands on subcycle timescales. *Nature* **2023**, *616*, 696–701.
- (30) Kohn, W. Periodic thermodynamics. *J. Stat. Phys.* **2001**, *103*, 417–423.
- (31) Matsyshyn, O.; Song, J. C.; Villadiego, I. S.; Shi, L.-k. Fermi-Dirac staircase occupation of Floquet bands and current rectification inside the optical gap of metals: An exact approach. *Phys. Rev. B* **2023**, *107*, 195135.
- (32) Iadecola, T.; Chamon, C.; Jackiw, R.; Pi, S.-Y. Generalized energy and time-translation invariance in a driven dissipative system. *Phys. Rev. B* **2013**, *88*, 104302.
- (33) Liu, D. E. Classification of the Floquet statistical distribution for time-periodic open systems. *Phys. Rev. B* **2015**, *91*, 144301.
- (34) Iadecola, T.; Chamon, C. Floquet systems coupled to particle reservoirs. *Phys. Rev. B* **2015**, *91*, 184301.
- (35) Hone, D. W.; Ketzmerick, R.; Kohn, W. Statistical mechanics of Floquet systems: The pervasive problem of near degeneracies. *Phys. Rev. E* **2009**, *79*, 051129.
- (36) Liu, D. E.; Levchenko, A.; Lutchyn, R. M. Keldysh approach to periodically driven systems with a fermionic bath: Nonequilibrium steady state, proximity effect, and dissipation. *Phys. Rev. B* **2017**, *95*, 115303.
- (37) Shirai, T.; Mori, T.; Miyashita, S. Condition for emergence of the Floquet-Gibbs state in periodically driven open systems. *Phys. Rev. E* **2015**, *91*, 030101.
- (38) Wang, F.; Chen, W.; Bao, C.; Lin, T.; Zhong, H.; Zhang, H.; Zhou, S. Light-field dressing of transient photoexcited states above the Fermi energy. *Phys. Rev. Lett.* **2025**, *134*, 146401.

- (39) Boschini, F.; Zonno, M.; Damascelli, A. Time-resolved ARPES studies of quantum materials. *Rev. Mod. Phys.* **2024**, *96*, 015003.
- (40) Mahmood, F.; Chan, C.-K.; Alpichshev, Z.; Gardner, D.; Lee, Y.; Lee, P. A.; Gedik, N. Selective scattering between Floquet–Bloch and Volkov states in a topological insulator. *Nat. Phys.* **2016**, *12*, 306–310.
- (41) Bao, C.; Zhong, H.; Fan, B.; Cai, X.; Wang, F.; Zhou, S.; Lin, T.; Zhang, H.; Yu, P.; Tang, P.; others Floquet-Volkov interference in a semiconductor. *Phys. Rev. B* **2025**, *111*, L081106.
- (42) Merboldt, M.; Schüler, M.; Schmitt, D.; Bange, J. P.; Bennecke, W.; Gadge, K.; Pierz, K.; Schumacher, H. W.; Momeni, D.; Steil, D.; others Observation of Floquet states in graphene. *Nat. Phys.* **2025**, *21*, 1093–1099.
- (43) Choi, D.; Mogi, M.; De Giovannini, U.; Azoury, D.; Lv, B.; Su, Y.; Hübener, H.; Rubio, A.; Gedik, N. Observation of Floquet–Bloch states in monolayer graphene. *Nat. Phys.* **2025**, *21*, 1100–1105.
- (44) Fragkos, S.; Fabre, B.; Tkach, O.; Petit, S.; Descamps, D.; Schönhense, G.; Mairesse, Y.; Schüler, M.; Beaulieu, S. Floquet-Bloch valleytronics. *Nat. Commun.* **2025**, *16*, 5799.
- (45) Bao, C.; Schüler, M.; Xiao, T.; Wang, F.; Zhong, H.; Lin, T.; Cai, X.; Sheng, T.; Tang, X.; Zhang, H.; Yu, P.; Sun, Z.; Duan, W.; Zhou, S. Manipulating the symmetry of photon-dressed electronic states. *Nat. Commun.* **2024**, *15*, 10535.
- (46) Fan, B.; De Giovannini, U.; Hübener, H.; Zhou, S.; Duan, W.; Rubio, A.; Tang, P. Floquet optical selection rules in black phosphorus. *Sci. Adv.* **2025**, *11*, eadw2744.
- (47) Tsuji, N.; Oka, T.; Werner, P.; Aoki, H. Dynamical band flipping in Fermionic lattice systems: an ac-field-driven change of the interaction from repulsive to attractive. *Phys. Rev. Lett.* **2011**, *106*, 236401.

- (48) Zhou, S.; Bao, C.; Fan, B.; Wang, F.; Zhong, H.; Zhang, H.; Tang, P.; Duan, W.; Zhou, S. Floquet engineering of black phosphorus upon below-gap pumping. *Phys. Rev. Lett.* **2023**, *131*, 116401.
- (49) Bao, C.; Wang, F.; Zhong, H.; Zhou, S.; Lin, T.; Zhang, H.; Cai, X.; Duan, W.; Zhou, S. Light-induced ultrafast glide-mirror symmetry breaking in black phosphorus. *ACS Nano* **2024**, *18*, 32038–32044.
- (50) Brode, W. R. The determination of hydrogen-ion concentration by a spectrophotometric method and the absorption spectra of certain indicators. *J. Am. Chem. Soc.* **1924**, *46*, 581–596.
- (51) Hu, Y.-Y.; Liu, Z.; Nam, K.-W.; Borkiewicz, O. J.; Cheng, J.; Hua, X.; Dunstan, M. T.; Yu, X.; Wiaderek, K. M.; Du, L.-S.; others Origin of additional capacities in metal oxide lithium-ion battery electrodes. *Nat. Mater.* **2013**, *12*, 1130–1136.
- (52) Liu, X.; Liu, J.; Qiao, R.; Yu, Y.; Li, H.; Suo, L.; Hu, Y.-s.; Chuang, Y.-D.; Shu, G.; Chou, F.; others Phase transformation and lithiation effect on electronic structure of  $\text{Li}_x\text{FePO}_4$ : an in-depth study by soft X-ray and simulations. *J. Am. Chem. Soc.* **2012**, *134*, 13708–13715.
- (53) Katsufuji, T.; Okimoto, Y.; Tokura, Y. Spectral weight transfer of the optical conductivity in doped Mott insulators. *Phys. Rev. Lett.* **1995**, *75*, 3497.
- (54) Gedik, N.; Yang, D.-S.; Logvenov, G.; Bozovic, I.; Zewail, A. H. Nonequilibrium phase transitions in cuprates observed by ultrafast electron crystallography. *Science* **2007**, *316*, 425–429.
- (55) Wang, Q. H.; Kalantar-Zadeh, K.; Kis, A.; Coleman, J. N.; Strano, M. S. Electronics and optoelectronics of two-dimensional transition metal dichalcogenides. *Nat. Nanotech.* **2012**, *7*, 699–712.

- (56) Zhong, H.; Cai, X.; Bao, C.; Wang, F.; Lin, T.; Chen, Y.; Peng, S.; Tang, L.; Gu, C.; Tao, Z.; Zhang, H.; Zhou, S. High harmonic generation light source with polarization selectivity and sub-100- $\mu\text{m}$  beam size for time- and angle-resolved photoemission spectroscopy. *Ultrafast Sci.* **2024**, *4*, 0063.
- (57) Jung, S. W.; Ryu, S. H.; Shin, W. J.; Sohn, Y.; Huh, M.; Koch, R. J.; Jozwiak, C.; Rotenberg, E.; Bostwick, A.; Kim, K. S. Black phosphorus as a bipolar pseudospin semiconductor. *Nat. Mater.* **2020**, *19*, 277–281.
- (58) Reimann, J.; Schlauderer, S.; Schmid, C.; Langer, F.; Baierl, S.; Kokh, K.; Tereshchenko, O.; Kimura, A.; Lange, C.; Gdde, J.; others Subcycle observation of lightwave-driven Dirac currents in a topological surface band. *Nature* **2018**, *562*, 396–400.
- (59) Neufeld, O.; Mao, W.; Hbener, H.; Tancogne-Dejean, N.; Sato, S. A.; De Giovannini, U.; Rubio, A. Time- and angle-resolved photoelectron spectroscopy of strong-field light-dressed solids: prevalence of the adiabatic band picture. *Phys. Rev. Res.* **2022**, *4*, 033101.
- (60) Neufeld, O.; Hbener, H.; De Giovannini, U.; Rubio, A. Tracking electron motion within and outside of Floquet bands from attosecond pulse trains in time-resolved ARPES. *J. Phys.: Condens. Matter* **2024**, *36*, 225401.
- (61) Teichmann, T.; Wigner, E. Sum rules in the dispersion theory of nuclear reactions. *Phys. Rev.* **1952**, *87*, 123.
- (62) Gusynin, V.; Sharapov, S.; Carbotte, J. Sum rules for the optical and Hall conductivity in graphene. *Phys. Rev. B* **2007**, *75*, 165407.
- (63) Thole, B.; Carra, P.; Sette, F.; van der Laan, G. X-ray circular dichroism as a probe of orbital magnetization. *Phys. Rev. Lett.* **1992**, *68*, 1943.

- (64) Park, S. T. Interference in Floquet-Volkov transitions. *Phys. Rev. A* **2014**, *90*, 013420.
- (65) Gradshteyn, I. S.; Ryzhik, I. M. *Table of integrals, series, and products*; Academic press, 2014.

# TOC Graphic

